Journal of King Saud University – Science 32 (2020) 423–432

Contents lists available at ScienceDirect

Journal of King Saud University – Science

journal homepage: www.sciencedirect.com

Original article

In-silico studies of some oxadiazoles derivatives as anti-diabetic compounds

Muhammad Tukur Ibrahim *, Adamu Uzairu, Gideon Adamu Shallangwa, Abdulqadir Ibrahim

Department of Chemistry Ahamadu, Bello University, P.M.B.1044, Zaria, Nigeria

ARTICLE INFO

Article history:
Received 27 February 2018
Accepted 25 June 2018
Available online 26 June 2018

Keywords:
QSAR
Molecular docking
Oxadiazoles
α-glucosidase
Anti-diabetic compounds

ABSTRACT

An in-silico study was performed to investigate the anti-diabetic activities of 27 Oxadiazoles derivatives. The anti-diabetic compounds were optimized using Density Functional Theory (DFT) method utilizing B3LYP version with 6-31G* basis set. Genetic Function Algorithm (GFA) was used to build four models. Model 1 was chosen as the best model, assessed and found to be statistically significant with LOF = 0.030552, R^2 = 0.9681, R^2_{adj} = 0.9567, Q^2_{CV} = 0.9364 and R^2_{pred} = 0.6969. The results of the molecular docking studies revealed that ligand 10, 13 and 15 have the highest docking scores of −9.9 kcal/mol among the co-ligands. This study has shown that the docking scores generated were in good agreement with the work reported by other researchers. The results of this study give room for designing new anti-diabetic compounds with better inhibitory activity against α-glucosidase, an enzyme that catalyzes the hydrolysis of carbohydrate to produce excess glucose.

1. Introduction

Type 2 Diabetes mellitus (T2DM) is a critical metabolic failure characterized by less insulin action and high blood glucose level (Kenchappa et al., 2017). T2DM Is referred to as the fastest worldwide threat to human health (Kavitha et al., 2017) and It leads to Kidney disease, blindness, and lower limb amputation (Datar and Deokule, 2014; Khan et al., 2014). According to World Health Organization, if action is not taken by 2030, there will be at least 350 million people in the world with T2DM (Taha et al., 2016a).

α -Glucosidase is an enzyme that catalyzes the hydrolysis of carbohydrate to produce excess glucose. It is located in the epithelium tissue of the small intestine (Taha et al., 2015). α -Glucosidase inhibitors are classes of medications used to treat T2DM by inhibiting α-glucosidase.

Heterocyclic compounds are organic compounds containing nitrogen, oxygen, and sulfur with numerous applications in the field of agriculture, pharmacy, and industries (Dua et al., 2011). Oxadiazoles are five-membered ring heterocyclic compounds containing oxygen and nitrogen atoms (Patel et al., 2010). A new derivative of 6-Hydroxyaurone Analogues has been reported as a potent anti-diabetic agent against α-glucosidase (Sun et al., 2017). A large number of compounds having 1, 3, 4-oxadiazole ring have been reported to be active anti-diabetic agents (Taha et al., 2017c). Apart from α-glucosidase inhibitors (Taha et al., 2018). Other biological activities have been reported for molecules having 1, 3, 4-oxadiazole ring which includes; anti-glycation (Taha et al., 2016b), anti-leishmanial (Taha et al., 2017b), and β-glucuronidase inhibitors (Taha et al., 2017a). New drugs are usually collected using trial and error methods, which are time-consuming and expensive.

With an increase in computational power, an in-silico study has led to the evaluation of new active drugs with a fewer side effect (Abdulfatai et al., 2017). Molecular docking studies have been conducted to predict the binding affinities of different compounds and to illustrate specific areas of interaction between the ligands and the receptor (Amit et al., 2014; Boukarai et al., 2017) and (Wang et al., 2016). The aim of this study was to investigate the anti-diabetic properties of oxadiazole derivatives via QSAR and molecular docking.

2. Materials and method

2.1. QSAR studies

2.1.1. Dataset collection

27 sets of Oxadiazoles compounds and their anti-diabetic activities against α-glucosidase were gotten from the literature

* Corresponding author.
E-mail address: muhdtk1988@gmail.com (M.T. Ibrahim).

Peer review under responsibility of King Saud University.

Production and hosting by Elsevier

https://doi.org/10.1016/j.jksus.2018.06.006
1018-3647/

Table 1
Shows the structures and the activity (pIC_{50}) of the Oxadiazoles derivatives.

S/No	Structures	pIC_{50}
1	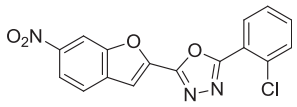	1.37
2	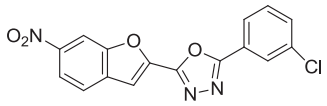	1.97
3	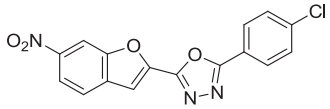	1.86
4	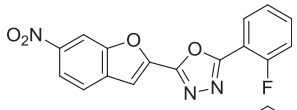	1.13
5	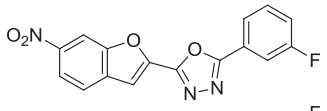	1.8
6	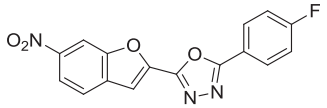	1.72
7	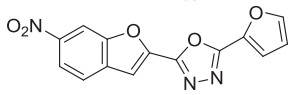	2.37
8	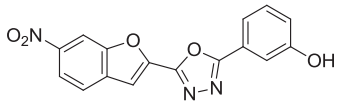	1.72
9	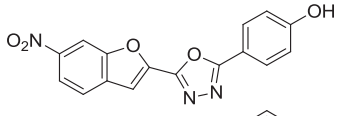	1.63
10	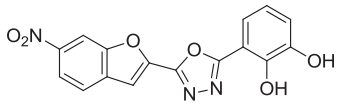	1.11
11	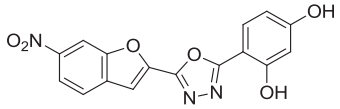	1.26
12	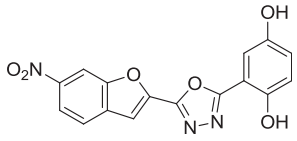	1.37
13	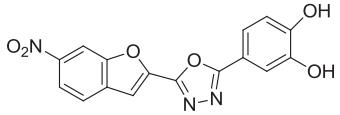	1.35
14	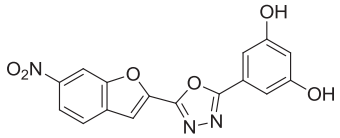	1.66
15	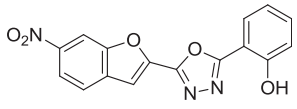	1.46

Table 1 (*continued*)

S/No	Structures	pIC_{50}
16	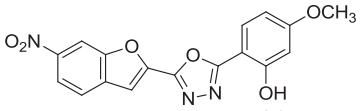	2.12
17	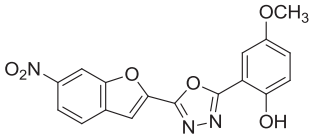	2.21
18	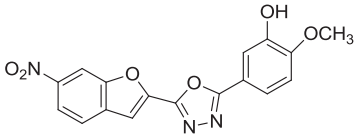	2.2
19	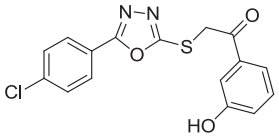	1.38
20	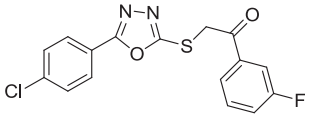	1.69
21	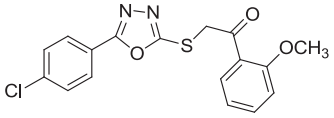	1.91
22	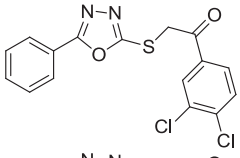	1.87
23	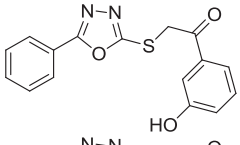	2.05
24	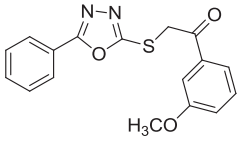	2.26
25	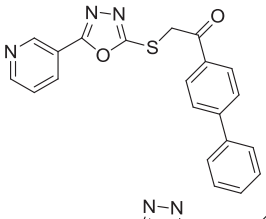	2.1
26	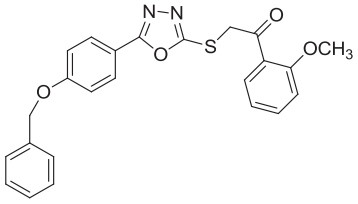	1.07
27	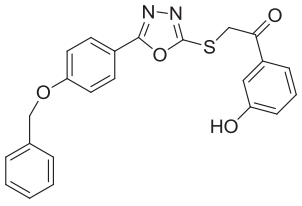	1.25

(Kashtoh et al., 2014; Taha et al., 2016b) and used for this study. The experimental activities of these compounds calculated as IC_{50} (μM) were convert to pIC_{50} ($pIC_{50} = \log 1/IC_{50}$). Table 1 shows the structures and the anti-diabetic activities of these molecules. The anti-diabetic activities of these molecules range from 1.07 to 2.37 (μM) as expressed in pIC_{50} logarithm scale.

2.1.2. Geometry optimization

ChemDraw Ultra version 12.0 software was used to draw the 2D structure of the compounds and save as cdx file format. The structures were then converted to 3D using Spartan 14.0 version 1.1.2 software. Density functional theory (DFT) using the B3LYP version and 6-311G* basis set, was employed for complete geometry optimization of the structures (Abdulfatai et al., 2016).

2.1.3. Molecular descriptors calculation

0D, 1D, 2D and 3D descriptors were calculated using PaDEL descriptor software version 2.18 and saved as sdf file format from the optimized structures of the Spartan files, (Yap, 2011).

2.1.4. Dataset division

Kennard–Stone Algorithm was used to split the dataset into training and test set using (Kennard and Stone, 1969). 75% of the dataset goes to the training set used and the remaining 25% as the test sets used for external validation of the built model.

2.1.5. Model building

Regression analysis was performed using Genetic Function Algorithm (GFA) method in material studio software with the biological activities (pIC_{50}) as the dependent variable and the physicochemical properties (descriptors) as independent variables.

2.1.6. Internal validations

The built models were assessed using Friedman's Lack of Fit (LOF) which served as a measure of fitness of a model. Below is the revised formula for the Friedman's lack of fit.

$$\mathrm{LOF} = \frac{\mathrm{SEE}}{\left(1 - \frac{C+dp}{M}\right)^2} \tag{1}$$

where SEE is the standard error of estimation, p is the total number of descriptors in the model, d is a user-defined smoothing parameter, c is the number of terms in the model, and M is the number compound in the training set.

SEE is the standard error of estimation which equals to the standard deviation of the model and a model is said to be good when it has lower SEE value. SEE is given as:

$$\mathrm{SEE} = \sqrt{\frac{(Y_{exp} - Y_{pred})^2}{N - P - 1}} \tag{2}$$

The structure of the regression model takes the form (Arthur et al., 2016):

$$Y = a_1x_1 + a_2x_2 + a_3x_3 + b \tag{3}$$

where Y is the biological activity (pIC_{50}), 'a's are regression coefficients for the corresponding 'x's which are the independent variables representing molecular descriptors of the molecules, the last variable 'c' is the regression constant.

R^2 gives an account of the fragment of total variation of the model. The closer the value of R^2 is to 1.0, the better the model generated. The most frequently used internal assessment parameter for QSAR model is R^2 and is shown below:

$$R^2 = 1 - \frac{\sum(Y_{exp} - Y_{prd})^2}{\sum(Y_{exp} - Y_{mntrng})^2} \tag{4}$$

where Y_{exp}, Y_{pred}, and $Y_{mntraining}$ are the observed activity, the predicted activity and the average observed activity of the training set (Adeniji et al., 2018).

Adjusted R^2 (R^2_{adj}) value changes directly with an increase in the number of descriptors; R^2 is not suitable for measuring the stability of a model. In order to have a reliable and stable model, R^2 needs to be adjusted. The adjusted R^2 is defined as follows:

$$R^2 = 1 - (1 - R^2)\frac{(n-1)}{n-p-1} = \frac{(n-1)(R^2 - P)}{n-p+1} \tag{5}$$

where n is the number of compounds in the training set, p = number of descriptors in the model (Abdulfatai et al., 2017).

The cross-validation coefficient (Q^2_{cv}) is used to determine the strength of a QSAR model to predict the activity of new compounds. Q^2_{cv} is represented as:

$$Q^2_{cv} = 1 - \frac{\sum(Y_{prd} - Y_{exp})^2}{\sum(Y_{exp} - Y_{mntrng})^2} \tag{6}$$

where Y_{pred} and Y_{exp} represent the predicted and experimental activity (pIC_{50}) respectively of the training set and Y_{mntrng} the average activity value of the training set (Jalali-Heravi and Kyani, 2004).

2.1.7. External validation

The external validation of the generated model is assessed based on the R^2 test value and is defined as:

$$R^2_{test} = 1 - \frac{\sum(Y_{prd} - Y_{exp})^2}{\sum(Y_{exp} - Y_{mntrng})^2} \tag{7}$$

where Y_{pred} and Y_{exp} represent the predicted and biological activity (pIC_{50}) respectively of the test set and Y_{mntrng} the mean activity value of the test set (Tropsha et al., 2003).

2.1.8. Applicability domain

Applicability domain of a QSAR model is employed to determine outliers and influential compounds and to affirm the reliability and robustness of the model generated (Tropsha et al., 2003). Leverage is one of the techniques used in evaluating the applicability domain of a QSAR model and is given for a chemical compound as h_i:

$$H_i = x_i(X^TX)^{-K}x_i^T(i = K, \cdots, P) \tag{8}$$

where x_i is the training compound matrix I, X is $n \times k$ descriptor matrix of the training set compounds and X^T is the transpose matrix X used to develop the model. As a prediction tool, the warning leverage (h^*) which is the limit for X values and it's defined as:

$$h^* = 3(p+1)/n \tag{9}$$

where n is the number of training compounds, and p is the number of descriptors in the model.

Table 2
General minimum recommended value for the evaluation of QSAR model.

Symbol	Name	Value
R^2	Co-efficient of determination	≥0.6
$P_{(95\%)}$	Confidence interval at 95% confidence level	<0.05
Q^2	Cross-Validation Co-efficient	≥0.5
R^2-Q^2	Difference between R^2 and Q^2	<0.3
$N_{(ext,\ \&\ test\ set)}$	Minimum number of external and test set	≥5
R^2_{ext}	Co-efficient of determination of external and test set	≥0.5

2.1.9. Quality assurance of the model

Internal and external validations parameters are used to assess the reliability and predictive ability of a QSAR model. Table 2 gives the general minimum requirement values for the assessment of a QSAR model (Veerasamy et al., 2011).

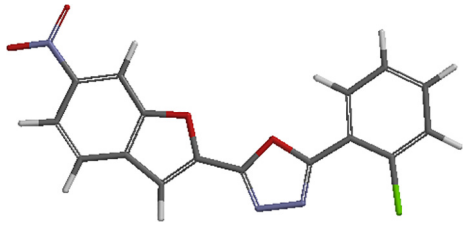

Fig. 1. 3D structure of the prepared ligand.

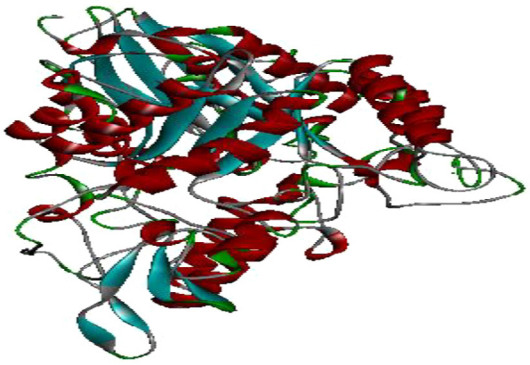

Fig. 2. 3D structure of the prepared receptor.

Table 3
List of the descriptors, their description, and classes for model 1.

S/No	Symbol	Description	Class
1	**AATS6s**	Average centered Broto-Moreau autocorrelation – lag 6/weighted by I-state.	2D
2	**ATSC3i**	Centered Broto-Moreau autocorrelation – lag 3/ weighted by first ionization potential	2D
3	**MATS1m**	Moran autocorrelation – lag 1/weighted by mass	2D
4	**VE3_Dt**	The logarithmic coefficient sum of the last eigenvector from detour matrix	2D
5	**JGI9**	Mean topological charge index of order 9	2D

2.2. Molecular docking studies

Protein-Ligand docking studies on 27 oxadiazoles derivatives were performed to study the interaction between the binding pocket of α-glucosidase enzyme and the ligands on Hp G62 computer system, with Intel ® Core™ i3 Dual CPU, M330 @2.13 GHz 2.13 GHz, 4 GB of RAM using Auto dock vina 4.2 of pyrex virtual screening software, Chimera version 1.10.2 and Discovery studio software.

2.2.1. Ligands preparation

The optimized structures of the compounds from Spartan'14 were saved as PDB file format for the docking studies (Abdulfatai et al., 2017). Fig. 1 shows the prepared structure of the ligand.

2.2.2. Preparation of receptor

The 3D structure of the receptor (Saccharomyces cerevisiae isomaltase) with the PDB code 3AJ7 was retrieved from Protein Databank (PDB). Discovery studio software was to prepare the receptor by removing water molecules and cofactors (Veerasamy et al., 2011) and save as PDB file format. Fig. 2 shows the prepared structure of the receptor.

2.2.3. Docking of the ligands with the receptor using autodock version 4.0 of pyrex software

The docking of ligands (oxadiazole derivatives) with the receptor (α-glycosidase) was done using Autodock version 4.0 of pyrex software (Trott and Olson, 2010). Chimera 1.10.2 software was used to build the complex (ligand-receptor) since the receptor and the ligand decoupled after carrying out docking with the autodock vina of pyrex. The ligand-receptor were visualized to view their interactions using Discovery studio visualizer.

3. Results and discussion

3.1. QSAR results of the Oxadiazoles derivatives

Genetic function algorithm of material studio software was used to generate four QSAR models. Out of these four models, model 1 was chosen as the best model based on its statistical significance as it has Friedman's Lack of fit value of 0.030552, the highest R^2 value of 0.9681, R^2_{adj} value of 0.9567, Q^2_{cv} value of 0.9364 and the R^2_{pred} value of 0.6969. The internal and external validation parameters of model 1 passed the minimum standard for a reliable QSAR model as given in Table 2.

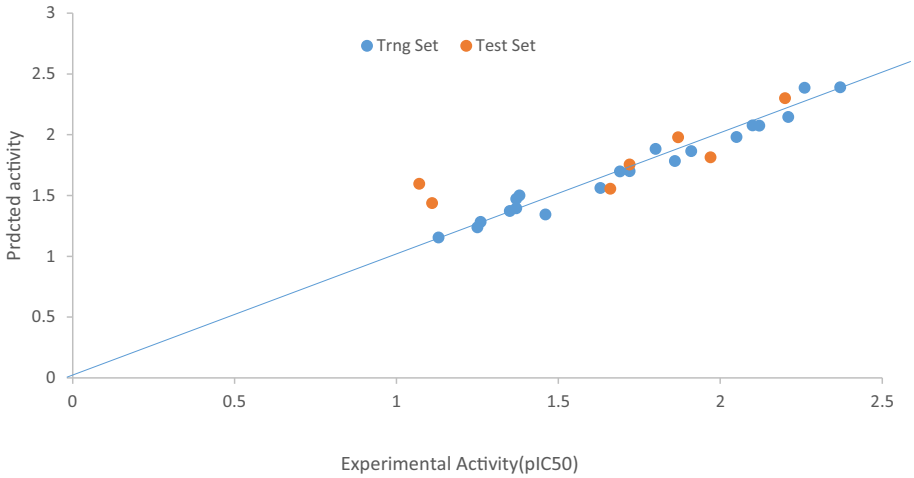

Fig. 3. The plot of the experimental and predicted activity of both the training and test sets of model 1.

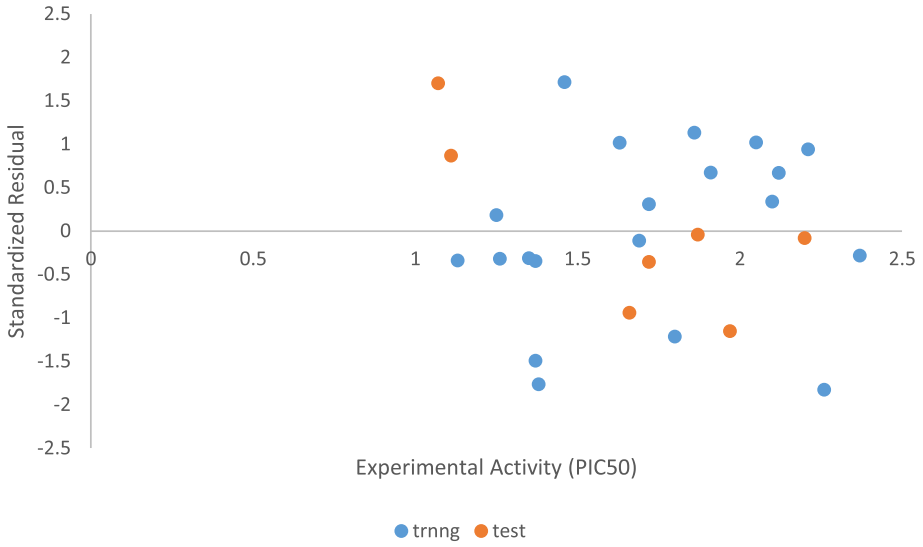

Fig. 4. The plot of standardized residual activity vs experimental activity.

Model 1

pIC_{50} = − 0.228309072 * **AATS6s** + 0.045721007 * **ATSC3i** + 9.007861457 * **MATS1m** + 0.110342533 * **VE3_Dt** + 61.318483952 * **JGI9** + 3.876735855.

LOF = 0.030552, R^2_{trng} = 0.968094, R^2_{adj} = 0.956699, Q^2_{LOO} = 0.936427, N $_{trng}$ = 20, R^2_{test} = 0.696907, N $_{test}$ = 7

The list of the descriptors, their descriptions, and classes for model 1 were presented in Table 3. The negative coefficients of the descriptor **AATS6s** mean that decrease in this descriptor will increase the anti-diabetic activity (pIC_{50}) against α-glycosidase enzyme. Furthermore, the Positive coefficient of **ATSC3i**, **MATS1m**, **VE3_Dt**, and **JGI9** descriptors implies that increasing such physiochemical parameters will increase the inhibitory activities of the Oxadiazole derivatives against α-glycosidase enzyme.

Fig. 3 shows the plot of predicted activities of both the training and the test sets against the experimental activities (pIC_{50}). We can see from the plot that the strength of the model was confirmed as the predicted R^2 value was in agreement with the R^2 value of 0.7085 extrapolated in the graph.

The random propagation of the standardized residuals on both sides of zero on Fig. 4 means that there was no systematic error in the built model. The experimentally determined activity correlates with the predicted activity as presented in Table 4. The Predicted activities and residuals of model 1 for the test set were presented in Table 5A. Table 5B shows the predictive R^2 of model 1 which confirmed its stability, reliability, and robustness.

Table 6 represents the correlation matrix of the descriptors of model 1 and found to be highly correlated which means that the descriptors used to build the model are very good.

The Williams plot of the standardized residuals against leverages is presented in Fig. 5. 3 influential compounds with S/No. 2, 6 and 26 were discovered from the plot and were part of the test set. It is evident that the influential compounds with leverages higher than the warning leverage h^*(h^* = 0.9) are structurally different from other compounds of the dataset.

Table 4
Comparison of observed (pIC_{50}), predicted (pIC_{50}) and residual of Model 1.

S/No	pIC_{50}	Predicted (pIC_{50})	Residual
1×	1.37	1.471973	−0.10197
3×	1.86	1.78263	0.07737
4×	1.13	1.153112	−0.02311
5×	1.8	1.883082	−0.08308
7×	2.37	2.389227	−0.01923
8×	1.72	1.698894	0.021106
9×	1.63	1.560508	0.069492
11×	1.26	1.281738	−0.02174
12×	1.37	1.393623	−0.02362
13×	1.35	1.371306	−0.02131
15×	1.46	1.342664	0.117336
16×	2.12	2.074292	0.045708
17×	2.21	2.145589	0.064411
19×	1.38	1.500609	−0.12061
20×	1.69	1.69746	−0.00746
21×	1.91	1.8639	0.0461
23×	2.05	1.980293	0.069707
24×	2.26	2.384813	−0.12481
25×	2.1	2.076754	0.023246
27×	1.25	1.237535	0.012465

x = training set.

3.2. Results of molecular docking studies of oxadiazole derivatives

Molecular docking studies on 27 Oxadiazole derivatives (inhibitors) against α-glycosidase (receptor) were carried out. All the ligands showed high docking scores (that is low energy values)

Table 5A
External validation of model 1.

S/No.	pIC_{50}	AATS6s	ATSC3i	MATS1m	VE3_Dt	JGI9	Y_{prd}	Y_{Prd} -Y_{obs}
2y	1.97	4.71789	−18.8368	0.027668	−8.88176	0.010406	1.845616	−0.12438
6y	1.72	5.846491	−19.4003	0.055399	−7.78663	0.007372	1.7468	0.0268
10y	1.11	5.015152	−23.047	−0.00592	−7.32121	0.010116	1.437137	0.327137
14y	1.66	5.328395	−23.0016	−0.00592	−6.73567	0.012715	1.591681	−0.06832
18y	2.2	4.454218	−20.2628	0.040483	−5.50237	0.009501	2.273457	0.073457
22y	1.87	3.477978	−24.438	0.011158	−4.58979	0.00739	2.012533	0.142533
26y	1.07	3.014347	−35.2293	0.070446	−10.1925	0.006678	1.497225	0.427225

y = testset

Table 5B
Calculation of the predictive R^2 of model 1.

S/No.	$(Yprd-Yobs)^2$	Ymntrng	Yobs-Ymntrng	$(Yobs-Ymntrng)^2$
2y	0.015471	1.7145	0.2555	0.06528
6y	0.000718	1.7145	0.0055	3.03E−05
10y	0.107019	1.7145	−0.6045	0.36542
14y	0.004667	1.7145	−0.0545	0.00297
18y	0.005396	1.7145	0.4855	0.23571
22y	0.020316	1.7145	0.1555	0.02418
26y	0.182521	1.7145	−0.6445	0.41538
	$\Sigma(Yprd-Yobs)^2 = 0.3361$			$\Sigma(Yobs-Ymntrng)^2 = 1.1089$

Therefore $R^2 = (1- \frac{0.3361}{1.1089}) = 0.6969$

Table 6
Pearson's correlation matrix of the descriptors in model 1.

	AATS6s	*ATSC3i*	*MATS1m*	*VE3_Dt*	*JGI9*
AATS6s	1				
ATSC3i	0.753534	1			
MATS1m	−0.30762	−0.36403	1		
VE3_Dt	0.077776	0.437029	−0.51926	1	
JGI9	0.523658	0.451096	−0.71465	0.157048	1

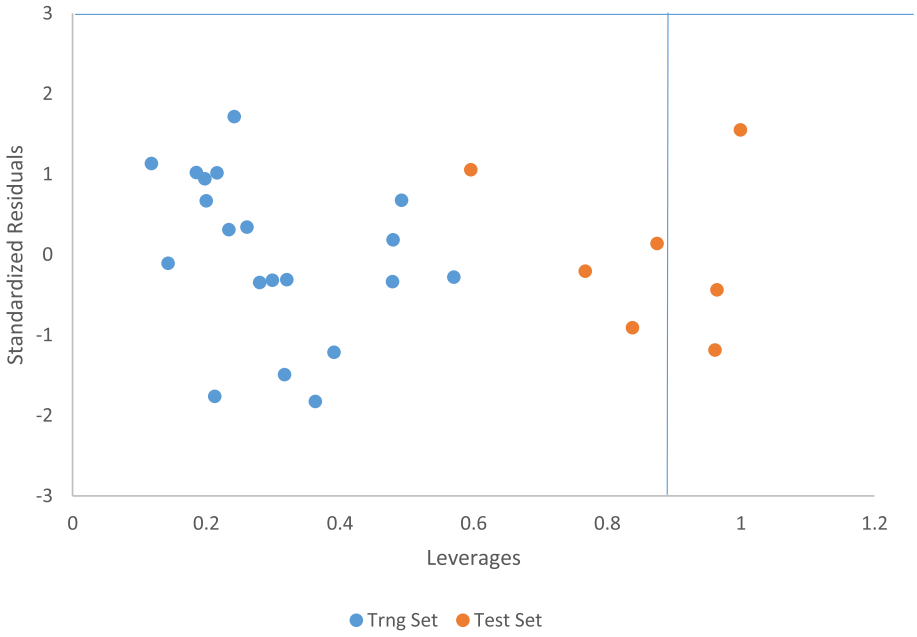

Fig. 5. Williams plot of the standardized residual and leverages of both the training and test.

which falls within the range of −8.2 to −9.9 kcal/mol as shown in Table 7. Ligands 10, 13 and 15 have the highest docking scores of −9.9 kcal/mol. Ligand 10 being among the ligands with the highest docking scores form 3 interactions: Hydrophobic, hydrogen bond, and carbon-hydrogen bond interactions. Hydroxyl groups of the phenyl ring of the ligand formed a hydrogen bond with Leu297 (2.2363 Å), Ser298 (2.2189 Å), Thr290 (2.4152 Å), Asp341 (2.0036 Å). Nitrogen 1 of the Oxadiazoles moiety formed a hydrogen bond with Ala292 (3.7179 Å). Arg263 form carbon-hydrogen bond with a nitrobenzofuran moiety of the ligand. The Ligand also formed hydrophobic interactions with the residues Ser291, Trp15, Ala292 and Arg263 as shown in Fig. 6A. Figs. 6B and 6C give the 3D and 2D structure of ligand 13 and 15.

3.3. Conclusion

An in-silico study was carried out on 27 Oxadiazoles derivatives as anti-diabetic compounds. Model 1 been the best was assessed internally and externally with Friedman's Lack of fit of 0.030552, squared correlation coefficient (R^2) of 0.9681, adjusted squared correlation coefficient (R^2_{adj}) value of 0.9567, Leave one out (LOO) cross-validation coefficient (Q^2_{CV}) value of 0.9364 and the external validation (R^2_{pred}) of 0.6969. Molecular Docking for this study revealed that ligand 10, 13 and 15 are the most active compounds having the highest docking scores of −9.9 kcal/mol. Ligand 10 being among the ligands with the highest docking scores form 3 interactions: Hydrophobic, hydrogen bond, and carbon-hydrogen bond interactions. Hydroxyl groups of the phenyl ring of the ligand formed a hydrogen bond with Leu297 (2.2363 Å), Ser298 (2.2189 Å), Thr290 (2.4152 Å), Asp341 (2.0036 Å). Nitrogen 1 of the Oxadiazoles moiety formed a hydrogen bond with Ala292 (3.7179 Å). Arg263 form carbon-hydrogen bond with a nitrobenzofuran moiety of the ligand. The Ligand also formed hydrophobic interactions with the residues Ser291, Trp15, Ala292 and Arg263. This research has shown that the binding affinity generated was in agreement with the work reported by other researchers (Taha et al., 2015) on this series of

Table 7
Binding energy, hydrophobic interactions, Electrostatic/other interactions, Hydrogen bonds and Hydrogen bond distance of α-glycosidase and the ligand.

Ligands	Binding Energy (kcal/mol)	Hydrophobic Interactions	Electrostatic/ Other Interactions	Hydrogen Bonds	Hydrogen Bond Distance (Å)
1	−9.5	TYR158, ARG315 and LYS156	ARG442 and GLU411	GLU411, ARG442 and ARG442	2.45988, 2.56427 and 2.39434
2	−9.6	ALA292, TRP15, TRP15 and ARG263		LEU297, ASN259, GLU296, LYS16 and LYS13	2.1837, 2.1989, 2.2826, 2.7578 and 3.0331
3	−9.4	TYR158, and LYS156	GLU411	GLU411, ARG442, ARG442 and SER240	1.9910, 2.6318, 2.4242 and 3.5081
4	−9.6	TYR158 and LYS156	ARG442, GLU411 and LEU313	GLU411, ARG315, ARG442, ARG442 and PHE314	2.3989, 2.3469, 2.5542, 2.4076 and 3.3223
5	−9.5	PHE178 and ARG315	ASP352 and ARG442	TYR158, GLU411, ARG442	2.5204, 2.9205 and 2.231
6	−9.5	PHE178 and ARG315	ASP352, ASP215, and GLU277	TYR158 and GLU411	2.5216 and 2.9019
7	−9.3	ALA292, TRP15 and ILE272		ASN259, GLU296, LYS16, and LYS13	2.1945, 2.4539, 2.8746 and 3.0918
8	−9.5	ALA292, TRP15, SER291, ALA292, ARG263 and ILE272		ASN259, GLU296, LEU297, SER298 and ARG292	2.35371, 2.6503, 2.4679, 2.9459 and 3.3034
9	−9.8	PHE178 and ARG315	ASP352	TYR158, GLU411 and GLU277	2.4532, 2.9738 and 2.8302
10	−9.9	ALA292, TRP15, SER291 and ARG263		LEU297, SER298, THR290, ASP341 and ALA292	2.2363, 2.2189, 2.4152, 2.0036 and 3.7179
11	−9.5	TYR158 and LYS156	GLU411	GLU411, LYS156, ARG442 and ARG442	1.9244, 2.3006, 2.6339 and 2.4430
12	−9.8	ALA292, TRP15, SER291, ARG263, ILE272 and ALA292		ASN259, ASN259, ARG270, LYS16, LYS13 and ILE272	2.5762, 2.3725, 2.0877, 2.2001, 3.2371 and 3.0425
13	−9.9	PHE178 and ARG315	ASP352	TYR158, GLU411, GLU277 and ARG442	2.5017, 2.9817, 2.3509 and 2.1559
14	−9.6	ALA292, TRP15 and ILE272		ASN259, GLU296, LYS16, and LYS13	2.3147, 2.5501, 2.7779 and 3.11320
15	−9.9	TRP15, SER291, ARG263, ILE272 and ALA292		ASN259, ASN259, LYS16, LYS13 and ILE272	2.5319, 2.2458, 2.1712, 3.2382 and 2.9205
16	−9.6	ALA292 and TRP15		ASN259, GLU296, LYS16, ARG270 and LYS13	2.2218, 2.3258, 2.8415, 3.7337 and 3.0338
17	−9.7	ALA292, TRP15 and ILE272		ASN259, GLU296, LYS16, GLU271, LYS13 and GLU271	2.4405, 2.8487, 2.8820, 3.4211, 3.1605 and 3.4816
18	−9.4	ILE272, ARG263, VAL266 and ALA292		GLU296, SER291, LEU297, ARG263, HIS295, GLU296, SER298 and ALA292	2.9749, 2.5521, 2.7170, 2.9698, 2.8341, 2.3460, 3.6410 and 2.9880
19	−8.9	ILE262, LYS13, ARG263, VAL266, ILE272, ALA292 and TRP15		GLU296, GLU296, ASN259 and LYS13	2.16198, 2.6436, 2.4589 and 3.7404
20	−8.9	ALA292, ARG263, VAL266, and TRP15		GLU296, GLU296, ARG263, and LYS13	2.2995, 2.8691, 3.0319 and 3.6105
21	−8.8	TYR158, VAL216 and PHE178	ASP352	TYR158, TYR158, GLU411 and SER157	2.8535, 2.6667, 2.7690 and 3.7598
22	−8.2	LYS156, ARG315, and TYR158		ASP242	2.77659
23	−9.1	TYR158, PHE178, and LYS156		TYR158, TYR158, GLU411, ASP242, SER241 and SER241	2.9085, 2.6097, 2.8659, 1.8365, 2.1041 and 2.2667
24	−8.9	ALA292, TRP15, ILE262, SER291, ARG263, VAL266 and ILE272		ASN259, GLU296, THR274 and SER298	2.2948, 2.1960, 2.8595 and 2.2601
25	−8.4	ILE262, ARG263 and VAL266	TRP15	GLU271, ILE272 and GLU296	2.5160, 1.9513 and 2.7252
26	−9.8	TYR158, TYR72, VAL216 and LYS156	ASP215 and GLU277	ASP307, ASP307 and GLU277	2.5099, 2.8113 and 3.1798
27	−9.6	VAL308, ARG315, TYR158 and LYS156		THR310 and THR310	2.3287 and 2.2118

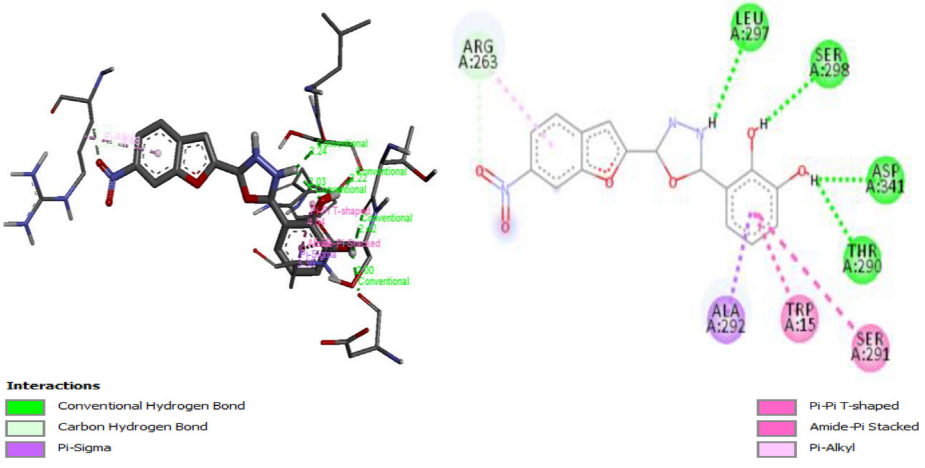

Fig. 6A. A3D and 2D structure of Ligand-Receptor complex 10 (−9.9 kcal/mol).

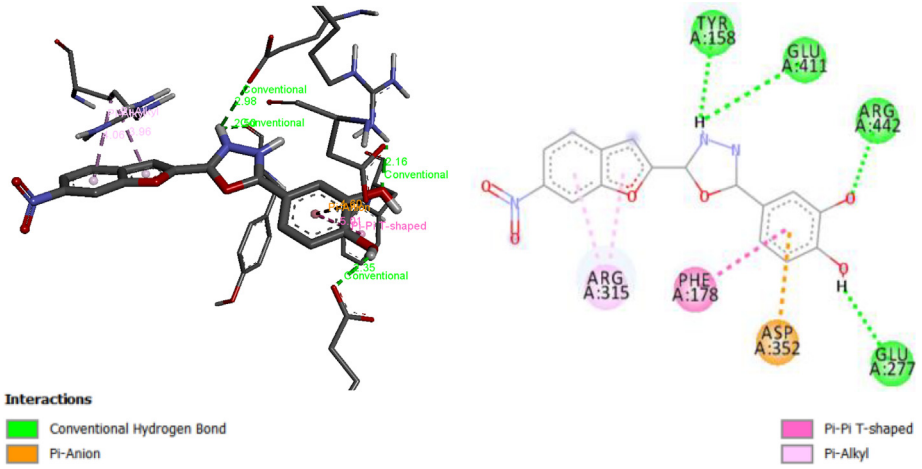

Fig. 6B. 3D and 2D structure of Ligand-Receptor complex 13 (−9.9 kcal/mol).

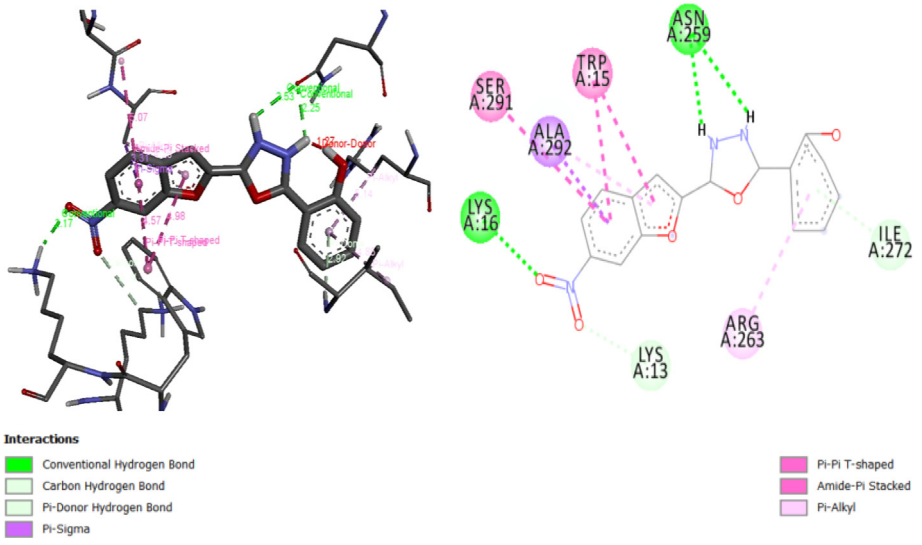

Fig. 6C. 3D and 2D structure of Ligand-Receptor complex 15 (−9.9 kcal/mol).

compounds. The QSAR and molecular docking results correspond with one another and give room for the design of new anti-diabetic compounds with better activity against α-glycosidase.

Acknowledgment

The authors sincerely acknowledge Ahmadu Bello University, Zaria for its technical support, Dr. Sani Uba and Abdulfatai Usman for their advice in the cause of this research.

References

Abdulfatai, U., Uzairu, A., Uba, S., 2016. In Silico Study Of Some Anticonvulsant Compounds. Scholars' Press. 978-3-330-65212-5.

Abdulfatai, U., Uzairu, A., Uba, S., 2017. Quantitative structure-activity relationship and molecular docking studies of a series of quinazolinonyl analogues as inhibitors of gamma amino butyric acid aminotransferase. J. Adv. Res. 8, 33–43.

Adeniji, S.E., Uba, S., Uzairu, A., 2018. Quantitative structure-activity relationship and molecular docking Of 4-alkoxy-cinnamic analogues as anti-mycobacterium tuberculosis. J. King Saud Univ. Sci.

Amit, C., Payal, C., R. K, D., 2014. Qsar Study Of 2,4-Dioxothiazolidine Antidiabetic Compounds.

Arthur, D.E., Uzairu, A., Mamza, P., Abechi, S.E., Shallangwa, G., 2016. Insilco study on the toxicity of anti-cancer compounds tested against molt-4 And P388 cell lines using Ga-Mlr technique. Beni-Suef Univ. J. Basic Appl. Sci. 5, 320–333.

Boukarai, Y., Khalil, F., Bouachrine, M., 2017. Qsar Study Of Flavonoid Derivatives As In Vitro Inhibitors Agents Of Aldose Reductase (Alr2) Enzyme. For Diabetic Complications.

Datar, P., Deokule, T., 2014. Design and synthesis of thiadiazole derivatives as antidiabetic agents. Med. Chem. 4, 390–399.

Dua, R., Shrivastava, S., Sonwane, S., Srivastava, S., 2011. Pharmacological significance of synthetic heterocycles scaffold: a review. Adv. Biol. Res. 5, 120–144.

Jalali-Heravi, M., Kyani, A., 2004. Use of computer-assisted methods for the modeling of the retention time of a variety of volatile organic compounds: a Pca-Mlr-ann approach. J. Chem. Inf. Comput. Sci. 44, 1328–1335.

Kashtoh, H., Hussain, S., Khan, A., Saad, S.M., Khan, J.A., Khan, K.M., Perveen, S., Choudhary, M.I., 2014. Oxadiazoles and thiadiazoles: novel α-glucosidase inhibitors. Bioorg. Med. Chem. 22, 5454–5465.

Kavitha, S., Kannan, K., Gnanavel, S., 2017. Synthesis, Characterization and biological evaluation of novel 2, 5 substituted-1, 3, 4 oxadiazole derivatives. Saudi Pharm. J. 25, 337–345.

Kenchappa, R., Bodke, Y.D., Chandrashekar, A., Sindhe, M.A., Peethambar, S., 2017. Synthesis of coumarin derivatives containing pyrazole and indenone rings as potent antioxidant and antihyperglycemic agents. Arabian J. Chem. 10, S3895–S3906.

Kennard, R.W., Stone, L.A., 1969. Computer aided design of experiments. Technometrics 11, 137–148.

Khan, K.M., Rahim, F., Wadood, A., Kosar, N., Taha, M., Lalani, S., Khan, A., Fakhri, M. I., Junaid, M., Rehman, W., 2014. Synthesis and molecular docking studies of potent α-glucosidase inhibitors based on biscoumarin skeleton. Eur. J. Med. Chem. 81, 245–252.

Patel, K., Jayachandran, E., Shah, R., Javali, V., Sreenivasa, G., 2010. Synthesis, characterization and anthelmintic activity (perituma posthuma) of new

oxadiazole incorporated with imidazole and pyrazole. Int. J. Pharma Bio Sci. 1, 1–14.
Sun, H., Ding, W., Song, X., Wang, D., Chen, M., Wang, K., Zhang, Y., Yuan, P., Ma, Y., Wang, R., 2017. Synthesis of 6-hydroxyaurone analogues and evaluation of their α-glucosidase inhibitory and glucose consumption-promoting activity: development of highly active 5, 6-disubstituted derivatives. Bioorg. Med. Chem. Lett. 27, 3226–3230.
Taha, M., Baharudin, M.S., Ismail, N.H., Selvaraj, M., Salar, U., Alkadi, K.A., Khan, K.M., 2017a. Synthesis and in silico studies of novel sulfonamides having oxadiazole ring: as β-glucuronidase inhibitors. Bioorg. Chem. 71, 86–96.
Taha, M., Imran, S., Rahim, F., Wadood, A., Khan, K.M., 2018. Oxindole based oxadiazole hybrid analogs: novel α-glucosidase inhibitors. Bioorg. Chem. 76, 273–280.
Taha, M., Ismail, N.H., Imran, S., Selvaraj, M., Jamil, W., Ali, M., Kashif, S.M., Rahim, F., Khan, K.M., Adenan, M.I., 2017b. Synthesis and molecular modelling studies of phenyl linked oxadiazole-phenylhydrazone hybrids as potent antileishmanial agents. Eur. J. Med. Chem. 126, 1021–1033.
Taha, M., Ismail, N.H., Imran, S., Wadood, A., Rahim, F., Saad, S.M., Khan, K.M., Nasir, A., 2016a. Synthesis, molecular docking and α-glucosidase inhibition Of 5-Aryl-2-(6′-Nitrobenzofuran-2′-Yl)-1, 3, 4-Oxadiazoles. Bioorg. Chem. 66, 117–123.
Taha, M., Ismail, N.H., Jamil, W., Imran, S., Rahim, F., Kashif, S.M., Zulkefeli, M., 2016b. Synthesis of 2-(2-Methoxyphenyl)-5-Phenyl-1, 3, 4-oxadiazole derivatives and evaluation of their antiglycation potential. Med. Chem. Res. 25, 225–234.
Taha, M., Ismail, N.H., Lalani, S., Fatmi, M.Q., Siddiqui, S., Khan, K.M., Imran, S., Choudhary, M.I., 2015. Synthesis of novel inhibitors of α-glucosidase based on the benzothiazole skeleton containing benzohydrazide moiety and their molecular docking studies. Eur. J. Med. Chem. 92, 387–400.
Taha, M., Rahim, F., Imran, S., Ismail, N.H., Ullah, H., Selvaraj, M., Javid, M.T., Salar, U., Ali, M., Khan, K.M., 2017c. Synthesis, α-glucosidase inhibitory activity and in silico study of tris-indole hybrid scaffold with oxadiazole ring: as potential leads for the management of type-Ii diabetes mellitus. Bioorg. Chem. 74, 30–40.
Tropsha, A., Gramatica, P., Gombar, V.K., 2003. The importance of being earnest: validation is the absolute essential for successful application and interpretation of Qspr models. Mol. Inf. 22, 69–77.
Trott, O., Olson, A.J., 2010. AutoDock Vina: improving the speed and accuracy of docking with a new scoring function, efficient optimization, and multithreading. J. Comput. Chem. 31, 455–461.
Veerasamy, R., Rajak, H., Jain, A., Sivadasan, S., Varghese, C.P., Agrawal, R.K., 2011. Validation of qsar models-strategies and importance. Int. J. Drug Des. Discov. 3, 511–519.
Wang, G., Peng, Z., Wang, J., Li, J., Li, X., 2016. Synthesis, biological evaluation and molecular docking study of N-arylbenzo [D] oxazol-2-amines as potential α-glucosidase inhibitors. Bioorg. Med. Chem. 24, 5374–5379.
Yap, C.W., 2011. Padel-descriptor: an open source software to calculate molecular descriptors and fingerprints. J. Comput. Chem. 32, 1466–1474.